

Integration of core-scale logging, dual-energy computed tomographic imaging and geochemical and mineralogical analysis of a composite core

Helene Velcin^{1,2*}, *Jeremie Dautriat*², *Lionel Esteban*², *Mark D. Lindsay*¹, *Annette D. George*¹, *Thomas Richard*³, *Adam Ramage*²

¹The University of Western Australia, School of Earth Sciences, WA 6009, Australia

²CSIRO Energy, Australian Resources Research Centre, Kensington, Western Australia 6076

³Epslog SA, 69 Jean Street, Hamilton Hill, 6163 WA, Australia

Abstract. Determining reservoir properties is challenging because it requires integration of data collected at different scales, from wireline measurements to sample powders analysed in laboratory. Low spatial resolution of well-log data (usually collected at ~50 mm intervals at best) and plug intervals (every 0.25–0.3 m) generates gaps between data points that may lead to over- or underestimate reservoir properties. The objective of this study is to measure different petrophysical properties, directly at the drill core-scale, to reduce the laboratory plug characterisation, as well as the gap between data points. Eleven different sandstones, three different limestones and a piece of granite were used to create a composite core of 10 cm in diameter and 84 cm long. The sandstones are homogeneous with distinct petrophysical properties from each other and were selected as appropriate analogues for oil and gas reservoirs. Sections of these sandstones, cut at different angles, were assembled to simulate realistic core heterogeneities with different: (i) rock types (texture, porosity and mineralogical variations), (ii) interface orientations between sandstones and (iii) fracture distribution. This study presents the integration of measurements obtained at different scales with core-scale logging techniques and dual energy (DE) method from X-ray imaging, supported with X-ray diffraction analysis and laboratory measurements to determine rock type, mineralogical composition, density and porosity variation along the composite core. These datasets may then be integrated with wireline log data (e.g. depth correction, porosity quality check, density and mineralogy log derivations) to facilitate selection of representative plug samples for more advanced analysis. The combination of 1D properties measured with core-scale logging techniques, and the 3D data obtained with the X-ray imaging technique, have the potential to generate 3D properties in future studies.

1 Introduction

Evaluation of the distribution of mineralogical, petrophysical and geomechanical properties of subsurface rocks is fundamental for geological modelling and reservoir production estimation. A large part of the data used to constrain 3D reservoir models originates from downhole wireline logging tools and core characterisation, by means of collecting data across multiple scale from indirect and direct measurements. Wireline logging gathers physical properties such as density, resistivity and gamma ray used for rock typing (distribution of clay content and permeable layers), depositional environment interpretation, well to well correlation, porosity distribution estimation, and prediction of hydrocarbon content [1, 2]. However, the data collected are only an indication/estimation of the reservoir properties because they are determined from indirect measurements. Moreover, they can be

discontinuous, caused by tool malfunction; and the depth of measurements, estimated from the tool speed, must be corrected as well as the effect of the mud filtration [3, 4, 5]. In order to calibrate, correct and validate these well log data and interpretation, it may be necessary to physically sample the core for further laboratory evaluation.

Laboratory data can be collected at different scales on the core. At meter scale, the X-ray medical CT scanner is commonly used as a non-destructive method to measure the density of the material and quickly identify the degree of sedimentological/stratigraphic heterogeneity and/or potential core damage. From the collected 3D images, a sampling strategy can be defined for further laboratory measurements to better constrain and calibrate well logs and reservoir model [6]. After plugging the core material, samples are then used to perform direct measurements of critical reservoir properties such as porosity, permeability and capillary pressure. Petrographical and mineralogical analyses are conducted on thin sections and powders.

* Corresponding author: Helene.Velcin@csiro.au

These local measurements remain difficult to upscale as uncertainties remain as to the representativeness of the tested material of a given facies at well or reservoir scales. In addition, temperature, pressure and fluid present at depth may affect the bulk rock properties such as porosity and permeability [1]. Uncertainties regarding representativeness of the laboratory dataset needs to be taken into account in assessing the reliability of 3D geological models and evaluation of the reservoir [7, 3, 8].

X-ray computed tomography (XCT) scanning is the only non-destructive technique able to image bulk density at high resolution ($\sim 100\mu\text{m}^3$) of whole cores in 3D [9]. In addition, recent developments on dual-energy XCT acquisition have proven able to provide bulk density and effective atomic numbers maps that can be used to calculate porosity and mineralogy variation along the core. The different methods used in this study include XCT, HyLogger-3, Multi-sensor core logger (MSCL-S), and Scratch test. These generate measurements, in a semi-automated manner, of mineralogical composition, bulk density, magnetic susceptibility, chemical elements, P and S-wave velocities, and rock strength. Most of these instruments produce continuous images of the core surface, and the MSCL-S permits the acquisition of ultraviolet (UV) fluorescence images. In this paper, we applied and integrated these methods on a composite core composed of homogeneous sandstones and limestones, pre-characterised in the laboratory. The use of a composite core is important to develop, test and validate the workflow presented here for future application to real core materials, and also for discussion of the limitations and uncertainties related to each technique.

2 Integrated workflow

The proposed approach for core-scale characterisation involves the following key steps summarised in Figure 1:

1. Creation of an “artificial” core, referred as composite core, using different homogeneous and well-described rock materials, with contrasting rock properties, distinct grain size or distinct mineralogy;

2. Petrophysical properties and mineralogical composition are determined in the laboratory on companion samples extracted from the same component materials;

3. Collection of petrophysical, physical, geomechanical, geochemical and petrographic data, along the core using different logging instruments such as the HyLogger-3, Multi-sensor Core Logger and the scratch test. All these techniques: (i) are non- or micro destructive; (ii) produce profiles (well log-like dataset) of rock properties along the core in a semi-automatic fashion and; (iii) acquire data at relatively high spatial resolution (every cm);

4. Dual-Energy XCT scan of the composite core and interpretation of logs and 3D maps of density and effective atomic numbers;

5. Combination of this technique with HyLogger and/or X-Ray Diffraction (XRD) data to convert density

3D maps into mineral composition (quantitative analysis) that can be used to recalculate grain density and porosity along the core (profile/3D maps).

5. Calibration and validation of the profile data against the dataset acquired from point 2 on companion samples.

Core preparation and operation and functionality of instruments are reported in the following sub-sections.

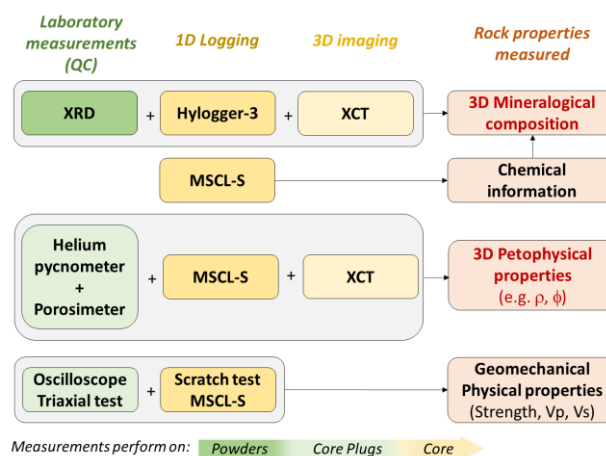


Fig. 1. Illustration of the integrated workflow and techniques used in this study to collect the rock properties of interest for core characterisation and our aim to ultimately create 3D models of these properties. Direct measurements are performed at core scale and validated using laboratory measurements performed on the analogue companion samples.

2.1 Core preparation and preliminary laboratory characterisation

To test the workflow, the composite core was composed of alternating rock materials extracted from blocks available in CSIRO’s core library. This approach allows use of companion samples for petrophysical and mineralogical characterisation. The composite core was created by cutting and assembling 18 pieces of cored material of 10cm in diameter. The selected rocks cover a large range of properties similar to actual petroleum reservoirs and are recognised as international reference materials. A total of 15 different materials were considered, covering mainly siliciclastic materials (including Berea, Nugget, Bentheimer, Crab Orchard, Idaho, Scioto, Colton, Carbon Tan, Castlegate, Kentucky and Boise sandstones, mostly extracted from deltaic deposits), a few calcareous materials (including Lueder, Mont Gambier and Savonnieres limestones) and a granite section at the base of the core (Figure A1). The total length of the synthetic core is 0.84 m. Some of the interfaces between material pieces were cut obliquely to the core axis to simulate tilted fractures and discontinuities, which were locally filled with clay (glaze). The different rocks used and their properties (porosity, permeability and uniaxial compressive strength) reported from the literature and the rock suppliers are listed in Figure A1 [10, 11, 12].

Petrophysical and mineralogical characterisation were performed on cylindrical samples (of 38 mm in diameter and ~80 mm in length) and powders extracted from each considered material block, respectively. Cylindrical samples and powders were dried for 48 hours at 105°C prior to testing. Bulk density (ρ_{bulk}) of the companion samples and grain density (ρ_{grain}), measured on powder sample with the Accupyc II 1340 helium pycnometer, were used to derive the total porosity (Φ). Compressional wave velocity (V_p) and shear wave velocity (V_s) were also measured on these plugs along the core length at ambient conditions. The mineralogical composition of the samples was determined by X-ray diffraction (XRD) and reported in Table A1.

2.2 1D properties logging

2.2.1 Petrophysical and chemical characterisation

Petrophysical properties were measured along the core every centimetre using a Multi-sensor core logger (MSCL-S), developed by Geotek accommodating cores up to 1.5 m long. The MSCL-S enables continuous and non-destructive logging of the core surface. The equipment available at CSIRO can be used for the following measurements (see further details in [13, 14]):

- *Gamma density* measures the bulk density profile based on gamma attenuation on approximately 5 mm with a low activity Cs-137 gamma ray source
- *Magnetic susceptibility* represents the type and amount of magnetic minerals in the sample. Data are collected with a point sensor of 10 mm diameter measuring approximately 1000 mm³ of the rock material at the core surface.
- *Primary wave travel times* are measured between two stainless steel ultrasonic transducers of 25 mm diameter placed on each side of the core. The thickness of the core, as determined by the P-wave travel path, is estimated at each measurement point using a contactless laser. The first P-wave arrival time is picked automatically and knowing the distance between both transducers, the P-waves velocity (V_p) can be computed.
- *A high performance X-Ray Fluorescence (XRF)* core scanner used for XRF spectroscopy on 100 mm² at the surface of the core and can analyse a large range of elements from Mg to U.

The cores were also imaged using the Geoscan V colour line-scan camera that captures visible and UV light sources. The core images are recorded at the same depth as other data measured and then useful for core description to locate the different facies.

2.2.2 Geomechanical/physical logs

The equipment developed by Epslog was used in this study to measure the rock strength, V_p and V_s profile along the core. This transportable bench test is able to perform measurements on cores from 20 mm up to 0.15 m in diameter and from 20 mm up to 1 m long. A

Polycrystalline Diamond Compact (PDC) cutter ~10 mm wide is used to scratch the core surface along its length while measuring the force/strength, amplitude and orientation on the blade. The movement/speed of the PDC along the core (~ few mm/s) and the cut depth (between 0.1 and 2 mm, depending on lithology) are both controlled and kept constant during the test. The blade is equipped with three strain gauge sets mounted along three axes recording the force applied. It is shown in the literature that the pure cutting force is directly correlated with Uniaxial Compressive Strength (UCS) values [15, 16, 17, 18]. A four-centimetre sensor equipped with an ultrasonic emitter of 50 kHz and a receiver, is measuring both V_p and V_s along the surface of the core. Due to the geometry of the core as assembled, and the discontinuities between each lithology, axial measurements were available on limited core sections only. To overcome this limitation, V_p and V_s were also measured manually perpendicular to the core axis.

2.2.3 Mineralogical logging

Mineralogical composition of the core was assessed using the HyLogger-3 at CSIRO, Perth. This equipment uses hyperspectral reflectance to identify a large range of minerals using three different spectrometers covering spectra from visible-near-infrared (VNIR), between 400 nm and 1000 nm, to shortwave-infrared (SWIR), from 1000 nm to 2500 nm, and to thermal infrared (TIR), from 6000 to 14,500 nm [19,20]. VNIR measures iron oxides, rare earth element minerals and SWIR measures mainly minerals such as hydrous silicate, carbonate and sulphate minerals. TIR is used to characterise anhydrous silicates such as quartz, feldspar, garnet, pyroxene, olivine, and hydrous silicate, sulphate and carbonate minerals [20, 21]. The sensor has a footprint of 12x8 mm that can record a 1D spectral profile at the core surface along the core axis. The measurements are acquired automatically every 4 mm with an overlap while the table is moving at 48 mm/s, which records twelve simultaneous spectra per second. The data were processed using “The Spectral Geologist” software (TSG®).

2.3 3D XCT imaging – Dual energy

The petroleum industry largely uses XCT technologies to describe core and study their properties. There are two methods of XCT imaging acquisition. The most common is XCT single energy for routine core characterisation. The core is scanned in preserved or unpreserved condition to visualise its internal structure (bedding, macro porosity/cavities, fossil content, bioturbation, or core damage such as fractures, drilling fluid invasion etc.) and compute the bulk density profile. The second and more rarely used XCT acquisition method relies on the use of dual energy (DE-XCT) which scans the same material under high and low power energy. In DE, two different physical effects are predominant [22]: At high energy (> 100 kV), the Compton scattering effect is dominant and sensitive to density of material whereas at low energy (< 100 kV), the photoelectric absorption effect is dominant

and sensitive to atomic number of the component material. This technique has been developed for medical application and is widely used for fluid flow visualisation studies. However, limited research has been published on the use of this technique for core-scale characterisation [23, 24, 25, 26, 27]. By combining these two physical effects, XCT attenuation images can be inverted into density (ρ_{bulk}) and effective atomic number (Z_{eff}) images [22, 23]. In this study, a new image segmentation method combining HyLogger-3/XRD data and DE-XCT images was also developed to improve the mineralogical and porosity quantification along the core in 3D.

A medical XCT scanner, Siemens SOMATOM definition AS, was used at CSIRO, Perth, on the composite core, with a helical acquisition (0.35 mm pitch and slice thickness of 0.6 mm) every 0.1 mm slice spacing under 80 kV and 140 kV (i.e. dual energy). DE-XCT was used to compute bulk density (ρ_b) and atomic number (Z_{eff}) following the method described by Wellington and Vinegar^[22] (1987) and refined by Siddiqui and Khamees^[23] (2004). The density and Z_{eff} derived from DE-XCT acquisition was calibrated using four standard samples, quartz, teflon, water and air. These standards were scanned before and after DE-XCT acquisition on the composite core to check for any potential drift of the scanner settings during scanning. Both standard samples and composite core XCT images were reconstructed using a sharp reconstruction kernel algorithm (H60s from Siemens) that has the advantage of enhancing the high spatial frequency information on images and correct beam hardening effect around the core, at the cost of degrading the signal-to-noise ratio on the XCT images. However, such noise can be drastically reduced using a Non-Local mean (NLM) filter.

The following workflow describes the different steps in DE-XCT image processing applied to the standard samples and core composite to retrieve its ρ_{bulk} , Z_{eff} and mineralogical composition profiles along the core axis.

1. Standard samples and composite core DE-XCT images (80kV and 140kV) were opened on Avizo© (Thermofisher).
2. A Non-Local Mean filter was applied to all the data to reduce noise.
3. The mean XCT attenuation values from each standard sample acquired at 80kV and 140kV before and after composite core XCT acquisition were extracted.
4. An inversion code, following the methodology described by Siddiqui and Khamees^[23] (2004), and calibrated from standard samples in point 3, converted the composite core DE-XCT images into ρ_{bulk} images set and Z_{eff} images set.
5. The mean ρ_{bulk} , mean Z_{eff} and within each image set was calculated on Avizo© to generate their profiles along the core axis.
6. A median filter was applied to each Z_{eff} image to reduce the noise created by the inversion code.
7. Z_{eff} images were segmented and converted into mineral phases, guided by the mineralogical

qualitative and quantitative analysis provided by the HyLogger-3 and XRD data respectively.

8. A porosity profile was computed from the bulk density and grain density derived from the mineral composition (point 7) and compared with porosity measured on the companion plug samples in the laboratory.

3 Results and discussion

3.1 Physical properties and chemical analysis (MSCL-S)

Figure 2a shows the results obtained with the MSCL-S with (a) the physical properties measured (ρ_{bulk} , V_p and magnetic susceptibility per unit volume K) compared to the measurements performed in laboratory. An excellent correlation is observed for the ρ_{bulk} collected in laboratory and the MSCL-S profile. As regards the V_p , the MSCL-S data are discontinuous due to the nature of the core. The magnetic susceptibility profile displays significant variation, especially for the Colton sandstone with a magnetic susceptibility greater than 20×10^{-5} SI, but also Idaho, Scioto, Kentucky and Boise sandstones with magnetic susceptibility values between 5×10^{-5} and 10×10^{-5} SI. Higher susceptibility values are associated with a lower quartz content and higher hematite and or mica/illite content.

An example of some elemental results obtained with the XRF MSCL-S sensor are reported in Figure 2b and c. Major elements Si, Ca, Fe and Al indicate the different composite core lithology. Siliciclastic rock types have a Si concentration higher than 0.5×10^6 ppm. Glazed sections can be dissociated from the siliciclastic rock types if Fe and Al concentrations are higher than 4×10^4 ppm and higher or equal to 2×10^5 ppm respectively. Finally, calcareous rock types are easily identifiable with Si concentrations lower than 0.5×10^6 ppm and Ca concentrations greater than 2.5×10^5 ppm. The K log can be used to discriminate sandstone rich in K feldspar, or potassic clays such as illite. Natural light and UV images of the whole core were obtained by rotating the core manually and stacking the obtained images. The UV light images enable identification of calcareous facies in the core. Calcite in these rock types fluoresces orange in Lueder and Savonnieres limestones, whereas calcite in Mt. Gambier limestone fluoresces white. It is known that calcite can fluoresce in different colours depending on mineral impurities^[28] such as metal cations (e.g. Mn) and/or rare earth elements (e.g. Y) present in the fluid during precipitation or diagenetic alteration of the minerals and/or cements.

In the case of non-composite cores, XRF analysis gives valuable information not only in terms of facies determination, but also on the presence of specific minerals that can affect the permeability such as clays or different cements.

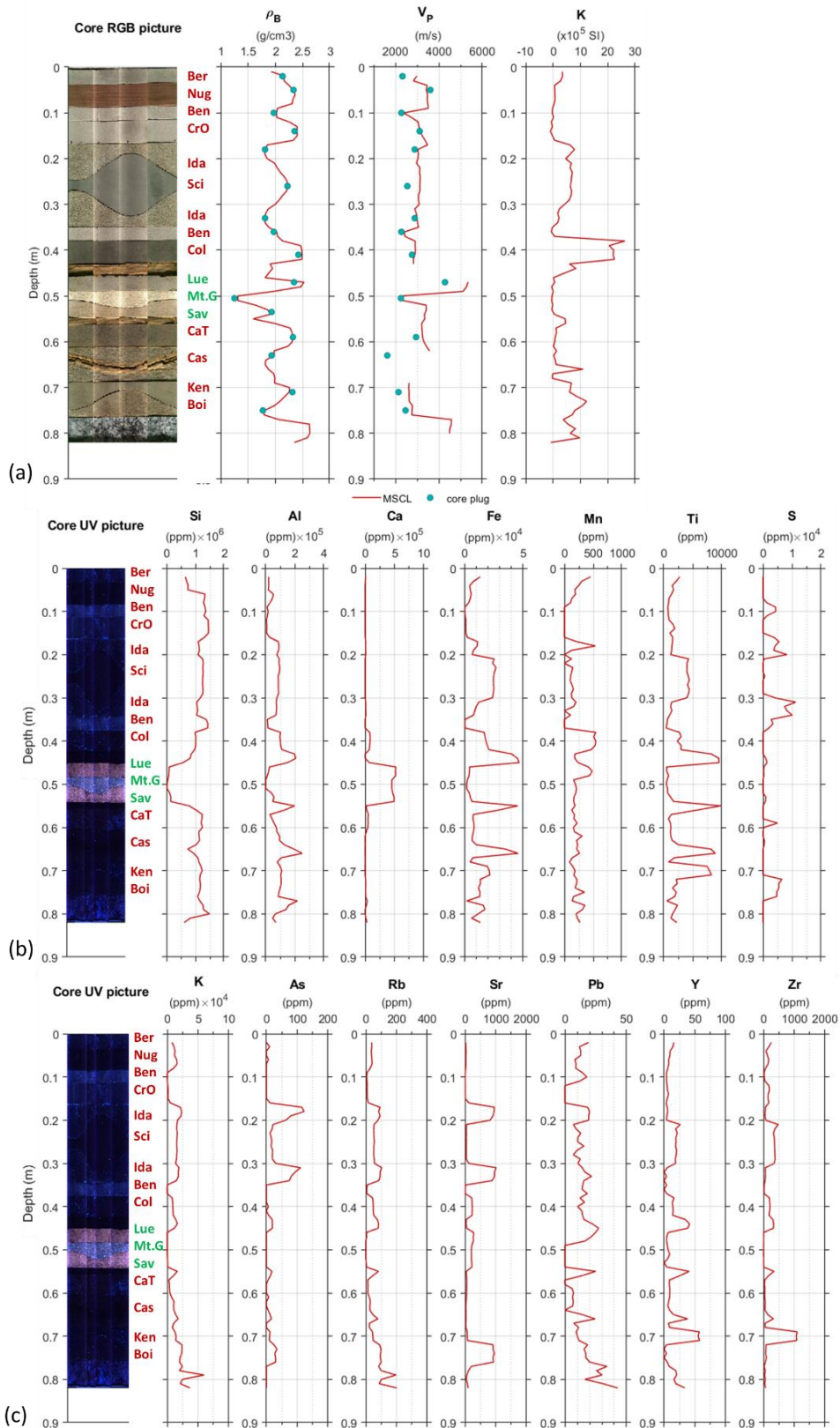


Fig. 2. Images, physical properties, and chemical analysis acquired with the MSCL-S. Image of the composite core acquired under natural and UV light. (a) Different physical property profiles measured along the core with ρ_{bulk} the gamma bulk density, V_p the P-waves and K the magnetic susceptibility. The laboratory measurements performed on the companion samples and powders for the bulk density and the V_p measurements are reported on the corresponding profiles (green filled circles). (b) and (c) Major and trace elements measured with the XRF sensor along the core.

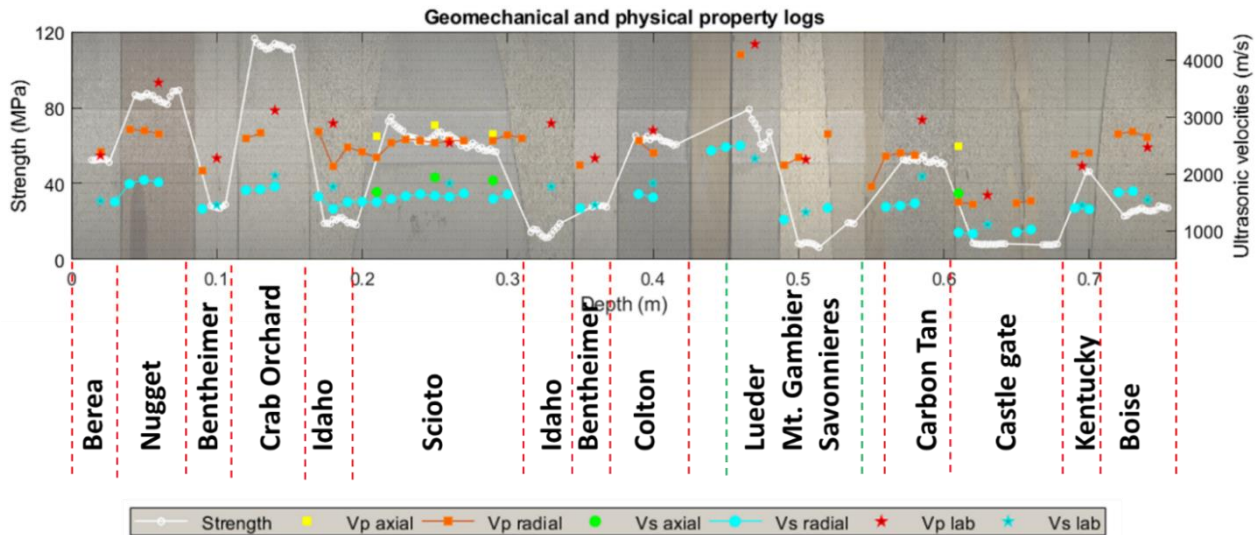


Fig. 3. Summary of the geomechanical and physical measurements generated by Epslog on the composite core using the scratch test and Vp -Vs sensors. In white high-resolution scratch test measurements (every 2mm); Vp (squares) and Vs (discs) were acquired in axial (yellow and green) and radial direction (orange and cyan) every 1 cm when the data acquisition was possible. Vp and Vs measurements performed on the companion samples are also reported in this figure (red and blue stars for Vp and Vs respectively).

3.2 Geomechanical and ultrasonic properties (Scratch test)

Figure 3 illustrates the strength, Vp and Vs data that were collected along the core with the scratch test. The strength data reported on the graph were collected every 2 mm whereas the Vp and Vs data were collected every 1 cm. Epslog's equipment measures ultrasonic velocities at the core sub-surface with a single sensor equipped with an emitter and a receiver. Note that the Vp, Vs and strength data were not measured on the granite base and glaze since these lithologies could not be analysed under the current equipment configuration.

The Vp and Vs data collected with the Epslog equipment (orange and cyan filled circles on the Figure 3) present the same trend as the data collected in laboratory (red and cyan stars), varying between 4250 and 1600 m/s for the Vp and between 2500 and 1000 m/s for the Vs. The strength (white circles) measured with the Scratch test gives a direct measurement of the UCS along the core. The UCS values obtained vary between ~9 and 120 MPa and are in accordance with the UCS data found in the literature or provided by the rock blocks suppliers (Figure A1, [10, 11, 12]).

UCS and elastic modulus are two critical parameters for determining mechanical properties of the rock, essential for well bore stability or reservoir subsidence studies. The scratch test has the unique advantage of providing continuous UCS profiles in a micro-destructive and cost-effective manner, avoiding the plug drilling process commonly undertaken for laboratory UCS measurements. It also provides ultrasonic velocity profiles along the core enabling the calculation of dynamic elastic moduli by combining these profiles and the density profile obtained with the MSCL-S (Medical XCT-scanner) equipment.

3.3 Mineralogical composition – qualitative analysis (HyLogger-3).

Figure 4 provides a comparative analysis of the XRD results introduced in the previous section and the HyLogger-3 measurements recorded in two orthogonal directions. The TSA library was used to process the data and the non-geological spectra were excluded from the dataset. The results obtained with the HyLogger-3 are consistent with the XRD data. The carbonate section has been well identified using the HyLogger-3. Silica/quartz, chlorite, sulfate, smectite and kaolin minerals in the sandstones were all recognized at their expected locations. However, note that kaolin was identified in the HyLogger-3 data in CrabOrchard but not via XRD. HyLogger-3 results indicate the presence of white micas where micas/illite was identified with the XRD analysis. The glazed sections are easily recognizable with the TIR spectrometer and are composed mostly of kaolinite with Na-feldspar and quartz. Na and K-Feldspar were only identified in the Idaho, Boise, and Kentucky sandstones where they represent more than 15% of the rock composition according to the XRD analysis. They were not detected in the other sandstones with a lower feldspar percentage. The Hylogger-3 results appear to be reliable, especially for rock type identification, although some caution is needed in terms of mineralogical identification. A complementary method such as XRD or scanning electron microscopy should be used for a quality check of the data and thus improving the reliability of this method.

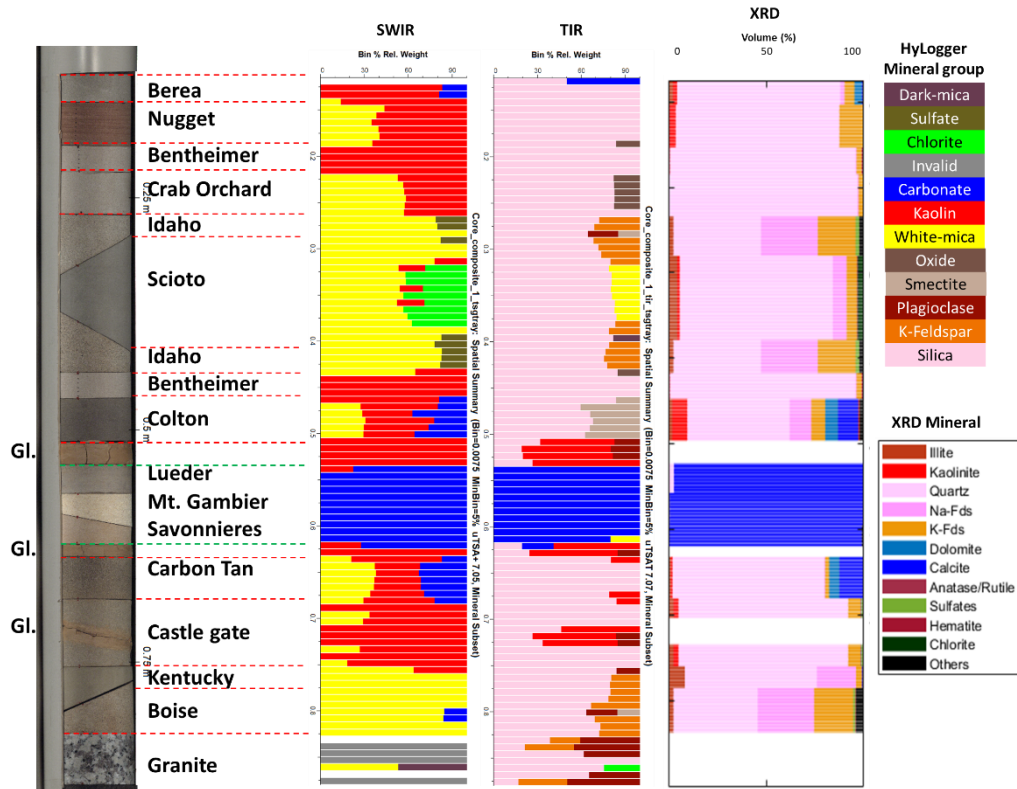


Fig. 4. Mineralogical qualitative analysis performed with the HyLogger-3 with TIR and SWIR spectrometer. The measurements were performed at the surface of the core. At the right end of the figure, the core-scale propagation of XRD results which are summarised in the Table A1 for comparison purpose with the HyLogger. Note that the granite base and the glaze sections were not analysed (corresponding to the four blank sections on the bar chart).

3.4 Petrophysical, physical properties and mineralogical composition 3D imaging (DE XCT)

The composite core picture, its 140kV post-filtered XCT image and the two properties ρ_b and Z_{eff} , derived from DE-XCT images on the composite core, are presented in map form, colour coded by intensity, as well as the mean profile (black line on Figure 5). These profiles clearly highlight the different rock types and their contacts along with some local heterogeneity.

Five different rock types are identified from Z_{eff} data and supported by HyLogger-3 mineralogy data (Figure 5 – Z_{eff} map): (i) sandstones composed mainly of quartz (in blue); (ii) sandstones rich in feldspars (in green); (iii) sandstone and glaze rich in calcite (green/yellow) which can be differentiated using the HyLogger-3 and/or MSCL-S data; (iv) limestone (in pink); (v) granite where the minerals are larger than the pixel size and characterized by very high bulk density.

For each rock type, ρ_{bulk} fluctuations are primarily related to fluctuation of porosities from one material to another. Porosity calculation is also dependent on the minerals present in each rock and requires a segmentation of each mineral, to compute the grain density, as described below. Both ρ_{bulk} and Z_{eff} maps are affected by area of high porosity in between each piece of rock composing the core. As highlighted on the profiles Figure 5, those discontinuities induce most of the time lower values of Z_{eff} , which is expected since the air Z_{eff} is 7.52^[23]. However, on both sides of the glazed sections

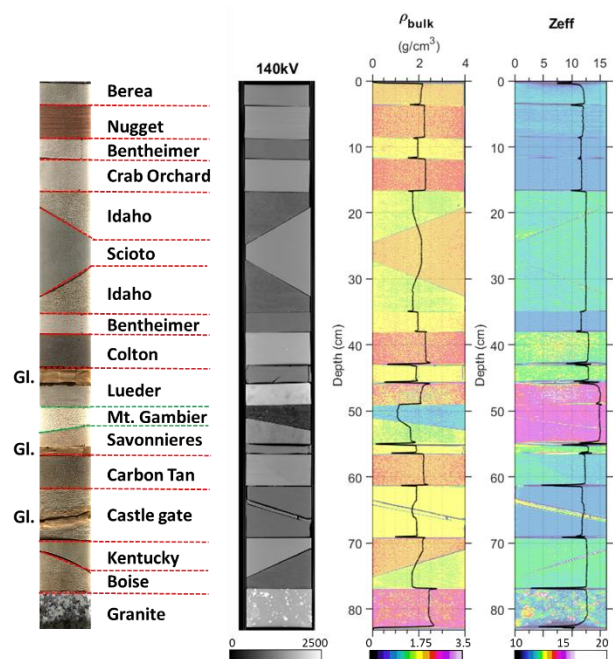


Fig. 5. Composite core image and rock types location (Gl. Sections correspond to the glaze), DE-XCT image and data from the composite core: from left to right: filtered raw XCT image acquired at 140kV; bulk density and Z_{eff} images colour labelled by intensity (their mean profiles is added in black line).

where the space between each piece is wider, artefacts with anomalously high Z_{eff} values are observable (Figure 5).

Note that such artefacts are not expected in the case of natural core that do not have such contrasting density values if undamaged.

Further to rock type identification, we proposed a segmentation of the Z_{eff} maps to quantify the mineralogical content along the core axis. This segmentation was calibrated and validated with HyLogger-3 and XRD data, respectively. Knowing the mineralogical composition of the core determined by HyLogger-3 and XRD, and by assuming that the minerals are “pure”, their corresponding/respective chemical formula was used to compute the Z_{eff} of each mineral constituting the composite core as follow:

$$Z_{eff} = \left(\sum f_i Z_i^n \right)^{\frac{1}{n}}, \quad (1)$$

with Z_i the atomic number of the i -th element and f_i the fraction of atoms of the i -th element in the mineral [23].

From XRD and HyLogger-3 data, the following minerals were considered for Z_{eff} segmentation: illite, kaolinite, Na-feldspar, quartz, K-feldspar, dolomite, calcite, rutile, anatase, natrojarosite and hematite. Their chemical formula and computed Z_{eff} from Eq.1 are summarized in Table 1.

Table 1. Minerals used for the composite core segmentation and their corresponding ρ_{grain} and calculated Z_{eff} from Eq. 1.

Mineral	Chemical Formula	Z_{eff}	ρ_{grain}
Illite	$KAl_3Si_3O_{10}(OH)_4$	9.6058	2.80
Kaolinite	$Al_2Si_2O_5(OH)_4$	11.1622	2.60
Na-Feldspar	$Na(AlSi_3O_8)$	11.5534	2.61
Quartz	SiO_2	11.7842	2.65
K-Feldspar	$KAlSi_3O_8$	13.3895	2.53
Dolomite	$CaMg(CO_3)_2$	13.7438	2.87
Calcite	$CaCO_3$	15.7100	2.71
Rutile	TiO_2	19.0006	4.20
Natrojarosite	$NaFe_3(SO_4)_2(OH)_6$	19.5642	3.09
Hematite	Fe_2O_3	23.4417	5.30

Figure 6 reports the results of two segmentation approaches to interpret the Z_{eff} maps, namely Thresholding #1 and Thresholding #2. The mineral segmentation (Thresholding #1: Figure 6) from Z_{eff} was achieved by defining Z_{eff} range for each identified mineral from HyLogger/XRD data. The computed Z_{eff} from Table 1 were first sorted in ascending intensity. For each mineral i , the threshold is centred on the Z_{eff} value and range from the mean value of the preceding ($i-1$) and considered mineral i , to the mean value of the following ($i+1$) and considered mineral i , as:

$$\frac{Z_{eff(i-1)} + Z_{eff(i)}}{2} < threshold(i) < \frac{Z_{eff(i+1)} + Z_{eff(i)}}{2}, \quad (2)$$

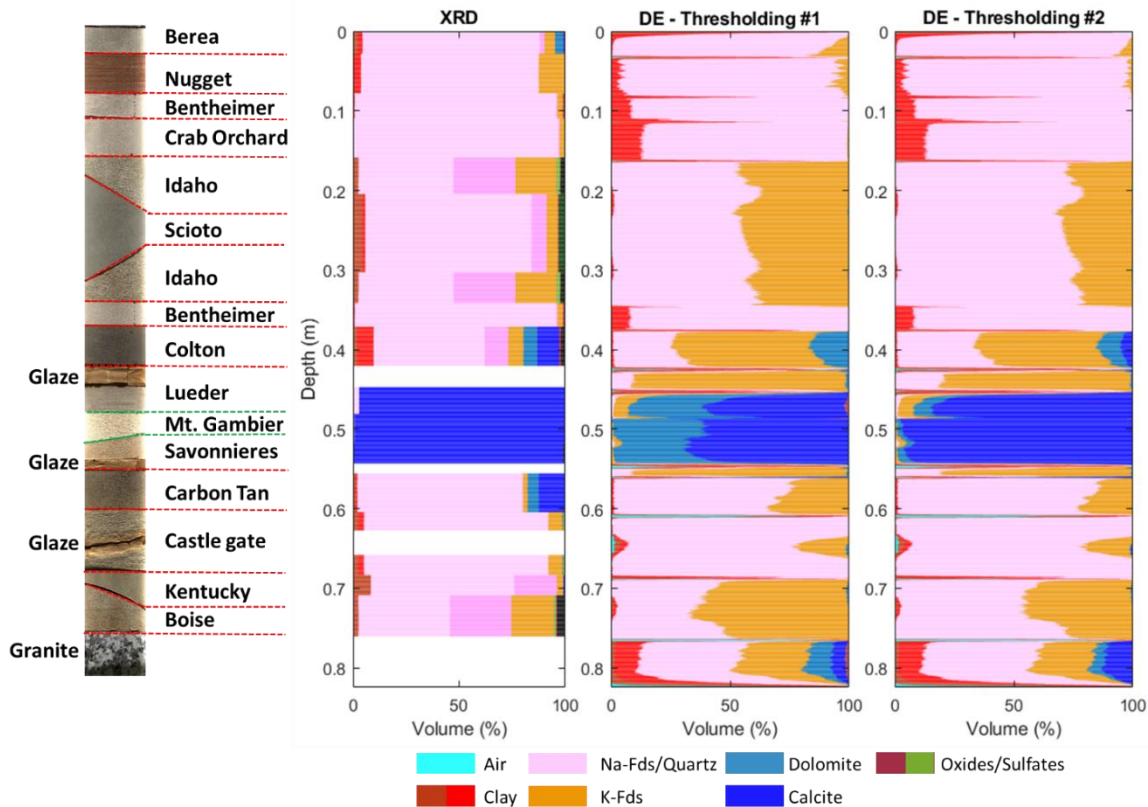


Fig. 6 Mineral composition along the composite core from XRD and DE-XCT. XRD analysis on a single sample extracted from each rock types of the composite core. DE-XCT mineralogy was computed from two threshold methods: (i) Basic mineral Z_{eff} boundaries and (ii) Improved Z_{eff} boundaries.

Due to their low contrast in Z_{eff} , Na-feldspar and quartz were segmented as a single mineral phase. The derived volume of each mineral in the different sandstones and limestones from Thresholding#1 was compared with XRD analyses (Figure 6). Overall, the result of the segmentation#1 is well correlated with the XRD data. However, some discrepancies remain observed, in terms of over- or under-estimation of some mineral phases. Kaolinite is overestimated in the vicinity of rock pieces edges, around the discontinuities described above, where only air or minerals such as quartz and feldspar are expected.

- Kaolinite is concentrated in some samples where it was measured with the HyLogger-3 but not with the XRD method.
- K-feldspar is overestimated in most sandstones such as Idaho, Scioto, Colton, Carbon Tan, Kentucky and Boise sandstones.
- Carbonate is also segmented and overestimated on both side of the glazed sections where anomalously high mean Z_{eff} values are observed. Calcite is underestimated in Colton, Carbon Tan sandstones and the limestone sections, where it is substituted by higher content in dolomite and/or K-Feldspar.

In order to improve the results of the Thresholding#1, a second segmentation was undertaken (Thresholding #2: Figure 6). The Z_{eff} mineral ranges were adjusted manually and calibrated against the XRD results. K-feldspar contribution is then successfully updated for the coarse sandstones Boise and Idaho but remains slightly overestimated in Scioto, Colton, Kentucky and

CarbonTan sandstones. All these sandstones are composed of fine grains, and are relatively tight with porosity values below 20%, low permeability (<5mD according to laboratory measurements), quartz content <80% and a high content in Fe and Ti for Scioto, Colton and Kentucky Sandstones (Table A1, Figure A1). The mineralogical diversity, the fine grain size and the resolution of the XCT scanner make difficult the segmentation of the different mineralogical phases, as the attenuation measured at the voxel size will more likely correspond to a mineral mixture than a single phase. The dolomite contribution remains unresolved in CarbonTan sandstone but was successfully improved in Colton sandstone, Lueder, Mt Gambier and Savonnières limestone sections. The remaining dolomite and K-Feldspar observed in the Lueder limestone may reflect a mixture of calcite and quartz. Note also that the segmentation used in this work is suitable for pure minerals having the chemical formula described in Table 1. However, in the case of chemical substitution or impurities in these minerals, Z_{eff} can be slightly different to those calculated from equation (2) and reported in Table 1. Finally, some remaining noise, after filtering, can also alter the quality of the segmentation and affect the resulting mineralogical content.

In conclusion, the combination of DE-XCT and HyLogger-3 scanning (quality checked with a few XRD points) appears to be a powerful method to determine the mineral composition and porosity changes along the core at high resolution and in 3D.

The porosity profiles, computed from the bulk density and grain density retrieved from mineralogical

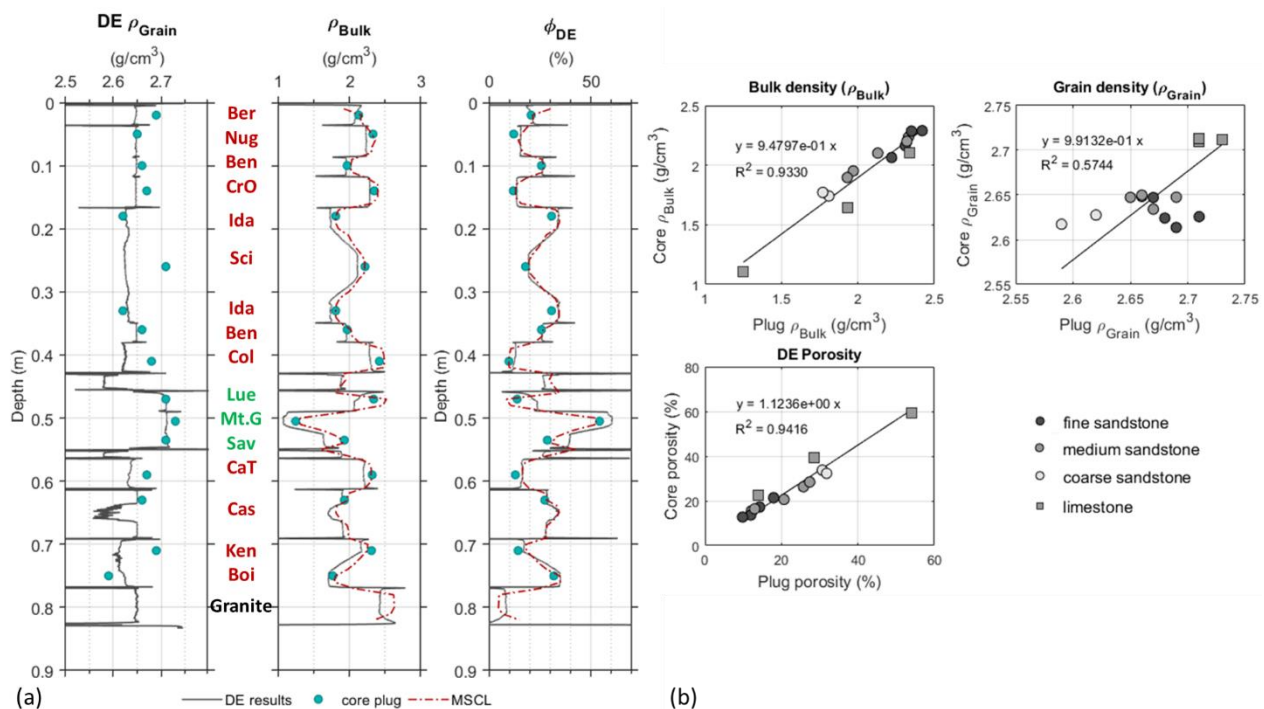


Fig. 7. (a) ρ_{grain} , ρ_{bulk} logs obtained with the DE methods using the second threshold and ρ_{bulk} measured with the gamma source on the MSCL-S are also reported on this plot for comparison purpose. Φ_{DE} calculated using both of the DE density and Φ_{DE} calculated using the DE ρ_{grain} and the gamma ρ_{bulk} . On each log are reported the measurements conducted in laboratory on the companion samples. (b) ρ_{bulk} , ρ_{grain} , and ϕ measured and calculated with the DE vs the measurements performed in laboratory on the companion samples.

composition along the composite core, is compared with porosity values inferred from different techniques (Figure 7). First, the bulk density derived from DE-XCT method is consistent with the bulk density measured with the MSCL-S gamma-density sensor, as well as those measured on companion samples in laboratory (green filled circles on Figure A5a, Figure A5b) with an excellent correlation factor. Grain density remains underestimated in Scioto, Colton, Kentucky and CarbonTan sandstone due to their characteristics described previously which impact the mineralogy segmentation (Figure 7a). Despite those grain density inconsistency values in tight samples, the porosity derived from DE-XCT is consistent with the laboratory porosity data with a coefficient of determination of 0.94 between the two datasets (Figure 7a, b).

4 Conclusion

Multiple datasets of petrophysical, geochemical, physical and mechanical properties and mineralogical composition of core extracted from exploration wells is essential for core characterisation, property interpretation and prediction of reservoir character. In this study, laboratory analyses were undertaken on plug samples to validate our workflow and methods. It has been shown that data acquired using different bench logging tools, in a non-destructive manner, matched conventional laboratory data. A full geochemical analysis was performed with the XRF sensor on the MSCL-S, supporting the mineralogical characterisation generated with the HyLogger-3 and the dual energy method. DE XCT imaging can be used to accurately determine the varying rock types of the composite core.

We demonstrate the relevance of DE-XCT scanning and core logging integration for : (i) rock typing, by capturing the proportion of minerals in each interval if the segmentation of the images is supported and constrained by HyLogger-3 or complementary local data such as XRD; (ii) bulk density and porosity calculation, (iii) collection of rock mechanical and acoustic velocities properties along the core. XCT scanning offers a unique opportunity to retrieve these properties along the core in 3D with a resolution of few 100s of micrometre. Future potential of this work is to build-up 3D models of the petrophysical, physical and mechanical properties by integrating 1D profiles and 3D models obtained using the different methods presented in this paper.

Acknowledgements

CSIRO Deep Earth Imaging Future Sciences Platform (DEI FSP) funded this research and provided a postgraduate scholarship, and UWA provided an international fees scholarship for HV. Dr Belinda Godel (CSIRO) is thanked for providing important advice to this project. Dr Ian Lau (CSIRO) is thanked for his help with HyLogger-3 data acquisition. This research utilized the X-ray medical CT, Hylogger-3 and Multi-sensor core logger at CSIRO, Kensington, Perth, as well as Epslog's

equipment. ML acknowledges support from MinEx CRC and ARC DECRA DE190100431.

References

1. S., Cannon, *Petrophysics: A Practical Guide*. John Wiley & Sons Incorporated, pp. 224. ISBN 978-1-118-74673-8 (2016)
2. E.J., Peters, *Advanced Petrophysics: Geology, Porosity, Absolute Permeability, Heterogeneity, and Geostatistics*. Vol.1, First Edition. ISBN: 978-1-936909-44-5 (2012).
3. W.R., Moore, Y.Z., Ma, J., Urdea, and T., Bratton, *Uncertainty Analysis in Well-Log and Petrophysical Interpretations*. In Y. Z. Ma and P. R. La Pointe, eds., *Uncertainty analysis and reservoir modelling: AAPG Memoir 96*, p. 17 – 28 (2011).
4. J.D., Walls, and M.B., Carr, *The Use of Fluid Substitution Modeling for Correction of Mud Filtrate Invasion in Sandstone Reservoirs*. SEG Technical Program Expanded Abstracts 2001: pp. 385-387. <https://doi.org/10.1190/1.1816624> (2001).
5. J.D., Walls, J., Dvorkin, M.B., Carr, *Well Logs and Rock Physics in Seismic Reservoir Characterization*. Offshore Technology Conference paper, Houston, Texas, U.S.A. (2004).
6. C., McPhee, J., Reed, I., Zubizarreta, *Core analysis: A best practice guide*. Elsevier, Developments in Petroleum Science 64 (United Kingdom). ISBN: 978-0-444-63533-4, ISSN: 0376-7361 (2015).
7. M.D., Lindsay, L., Ailleres, M.W., Jessell, E.A., de Kemp, P.G., Betts, *Locating and quantifying geological uncertainty in three-dimensional models: Analysis of the Gippsland Basin, southern Australia*. *Tectonophysics* 546-547, pp. 10-27. doi:10.1016/j.tecto.2012.04.007 (2012).
8. Z., Rui, J., Lu, Z., Zhang, R., Guo, K., R., Ling, Zhang, S., Patil, *A Quantitative Oil and Gas Reservoir Evaluation System for Development*, vol. 42. pp. 31–39 (2017).
9. F., Mees, R. Swennen, M., Van Geet, P., Jacobs, *Applications of X-ray computed tomography in the geosciences*. Geological Society, London, Special Publications 2003, v.215;p1-6 (2003)
10. Kocurek Industries INC. <https://kocurekindustries.com/>
11. V., Mikhailsevitch, M., Lebedev, and B., Gurevich, *Low-frequency laboratory measurements of the acoustic parameters of Savonnières limestone*. SEG Denver 2014 Annual Meeting, 2978-2982. DOI <http://dx.doi.org/10.1190/segam2014-1500.1> (2014).
12. Stone Contact <https://www.stonecontact.com/>
13. GEOTEK, *Documentation for the GEOTEK Multi-Sensor Core Logger (MSCL)*. Available online at: <https://www.geotek.co.uk/wp-content/uploads/2016/04/MSCL-manual-1-Nov-16.pdf> (version Nov 1, 2016)
14. A., Vatandoost, P., Fullagar, and M., Roach, *Automated Multi-Sensor Petrophysical Core Logging*, *Exploration Geophysics*, 39, 181-188 (2008).

15. S., Doshvarpassand, *Investigation into the impacts of rock/cutter interface geometry on drilling response of PDC cutters*. P.h.D. thesis. Curtin University (2017).
16. T., Richard, *Determination of rock strength from cutting tests*. Master of Science thesis. University of Minnesota, Minneapolis, Minnesota, USA (1999)
17. T., Richard, E. Detournay, A. Drescher, P. Nicodeme, D. Fourmaintraux, et al., *The scratch test as a means to measure strength of sedimentary rocks*. In *SPE/ISRM Rock Mechanics in Petroleum Engineering*. Society of Petroleum Engineers (1998)
18. T., Richard, F. Dagrain, E. Poyol, and E. Detournay. *Rock strength determination from scratch tests*. *Engineering Geology* 147, 91_100 (2012).
19. D.W., Coulter, X., Zhou, L.M., Wickert, P.D., Harris, *Advances in Spectral Geology and Remote Sensing: 2008-2017*. In "Proceedings of Exploration 17: Sixth Decennial International Conference on Mineral Exploration", p. 23–50(2017).
20. M. C., Schodlok, L., Whitbourn, J., Huntington, P., Mason, A., Green, M., Berman, D., Coward, P., Connor, W., Wright, M., Jolivet, R., Martinez, *HyLogger-3, a visible to shortwave and thermal infrared reflectance spectrometer system for drill core logging: functional description*, *Australian Journal of Earth Sciences*, 63:8, 929-940 (2016).
21. P., Mason, and J.F., Huntington, *HyLogger 3 components and pre-processing: An overview*. Northern Territory Geological Survey, Technical Note 2012-002 (2012).
22. S., Wellington, and H., Vinegar, *X-ray computerized tomography*. *Journal of Petroleum Technology*, 39(08), 885-898. <https://doi.org/10.2118/16983-PA> (1987).
23. S., Siddiqui, A.A., Khamees, S., Aramco, *Dual-Energy CT-scanning application in rock characterization*. Paper presented at the SPE Annual Technical Conference and Exhibition held in Houston, Texas, U.S.A., 26-29 September (2004).
24. J., Walls, and M., Armbruster, *Shale Reservoir Evaluation Improved by Dual Energy X-Ray CT Imaging*. *Journal of Petroleum Technology*, Vol.64, 28-32 (2012).
25. H., Al-Owihan, M., Al-Wadi, S., Thakur, S., Behbehani, N., Al-Jabari, M., Dernaika, S., Koronfol, *Advanced Rock Characterization by Dual Energy CT Imaging: A Novel Method in Complex Reservoir Evaluation*. 10.2523/IPTC-17625-MS (2014).
26. M.,Dernaika, Y., Naseer Uddin, S., Koronfol, O., Al Jallad, G., Sinclair, Y., Hanamura, K., Horaguchi, *Multi-Scale Rock Analysis for improved characterization of complex carbonates*. SPE-175598-MS, (2015)
27. R. A., Victor, M., Prodanovic, and C., Torres-Verdin, *Monte Carlo approach for estimating density and atomic number from dual-energy computed tomography images of carbonate rocks*. *Journal of Geophysical Research: Solid Earth*, 122, 9804–9824. <https://doi.org/10.1002/2017JB014408> (2017).
28. Geology page, *Florescence: Why Minerals Fluoresce?* (2020)
<http://www.geologypage.com/2020/03/fluorescence-why-minerals-fluoresce.html>

Appendix

Table. A1. Summary of the mineralogical quantitative analysis of the different formation used to create the composite core. These analyses were performed using the XRD technique on rock powders. (Qz.= quartz, Dolo.= dolomite, Natro.= natrojarosite, Hem.=hematite, Smec.=smectite, Chl=chlorite, Micro.=microcline, Orth.=orthoclase).

Sample	Qz.	Calcite	Dolo	Natro.	Mica/ Illite	Hem.	Kaolin	Smec.	Chl.	Albite	Micro.	Orth.	Zeolite	Anatase/ Rutile
	%	%	%	%	%	%	%	%	%	%	%	%	%	%
Berea	83.4	0.4	3.8		2.3	0.4	2.2			2.3	5.0			0.2
Nugget	83.7				0		3.8			0	12.2			
Bentheimer	95.0					1.1	0.8			0.5	2.6			
Crab Orchard	96.8					0.2				0.5	2.5			
Idaho	44.8			1.9	2.6					29.1	8.4	10.9	2.2	
Scioto	78.3				4.5		1.3		2.9	7.1	2.2	3.1		0.4
Colton	52.4	10.3	6.5		2.0	0.8	7.7	2.0		11.1	7.1			
Lueder	2.9	97.1												
Mt. Gambier	0.6	99.4												
Savonniere		99												
CarbonTan	77.7	12.0	5.2		1.2	0.4	0.9			0.4	2.1			
Castlegate	86.8	0.2		0.9	2.6	0.2	2.6				2.6	4.0		
Kentucky	67.6	0.4			8.4					20.0	1.8	1.3		0.5
Boise	43.1			1.1	2.6	0.4				28.9	7.8	12.2	3.9	



Fig. A1. Composite core and description of the analogue sandstones and limestones used to create the core. The porosity, permeability and uniaxial compressive strength (UCS) reported here are the ones provided by the rock suppliers or extracted from the literature [10, 11,12]